Off-line Flux Injection Test Probe for Screening Defective Rotors in Squirrel Cage Induction Machines

Jeong, M, Yun, J, Park, Y, Lee, SB & Gyftakis, KN

Original citation & hyperlink:
Jeong, M, Yun, J, Park, Y, Lee, SB & Gyftakis, KN 2018, 'Off-line Flux Injection Test Probe for Screening Defective Rotors in Squirrel Cage Induction Machines' *IEEE Transactions on Industry Applications*, vol (in press), pp. (in press)
https://dx.doi.org/[DOI]

DOI [DOI]
ISSN 0093-9994
ESSN 1939-9367

Publisher: IEEE

Quality Assurance Testing for Screening Defective Aluminum Die-cast Rotors of Squirrel Cage Induction Machines

Myung Jeong, Jangho Yun, Yonghyun Park, Sang Bin Lee
Department of Electrical Engineering,
Korea University, Seoul, Korea
sangbinlee@korea.ac.kr

Konstantinos Gyftakis
School of Computing, Electronics, and Mathematics
Coventry University, Coventry, United Kingdom

The recent trend in squirrel cage induction motor manufacturing is to replace fabricated copper rotors with aluminum die-cast rotors to reduce manufacturing cost to stay competitive in the global market. Porosity in aluminum die-cast squirrel cage rotors is inevitably introduced during the die cast process. Porosity can cause degradation in motor performance and can lead to a forced outage causing irreversible damage in extreme cases. Many off-line and on-line quality assurance test methods have been developed and applied for assessment of rotor quality. However, years of experience with the existing test methods revealed that they are not suitable for quality testing or capable of providing a quantitative assessment of rotor porosity with sufficient sensitivity. In this paper, a new off-line test method capable of providing sensitive assessment of rotor porosity is proposed. It is shown that rotors with minor and distributed porosity that are difficult to detect with other tests can be screened out during manufacturing. The proposed method is verified through a 3 dimensional finite element analysis and experimental testing on closed and semi-open slot aluminum die cast rotors of 5.5 kW induction motors with porosity.

Keywords - Aluminum Die-cast Rotor, Fault Detection, Fill Factor; Induction Machines, Porosity, Quality Assurance, Squirrel Cage Rotor

I. INTRODUCTION

The rotor is an important component of squirrel cage induction machines that determines the motor starting characteristics and operating efficiency [1]. Many motor manufacturers are replacing fabricated copper rotors with aluminum (Al) die-cast rotors, as they allow flexible rotor bar shape for design optimization and up to 20% reduction in motor cost compared to that of fabricated copper rotors. Leading motor manufacturers are employing Al die cast rotors for motors rated up to 800-900 kW for cost-competitiveness in the global market. There are a number of defects that can be introduced in Al die cast rotors during manufacturing such as porosity or blowholes that can degrade motor performance and reliability [1]-[4].

Porosity in Al die cast rotors, shown in Fig. 1(a), is inevitable during the manufacturing stage as Al shrinks by 6% in volume when molten aluminum is cooled, and there also can be insufficient injection of Al or leakage of Al during the die cast process [1]-[3]. The increase in rotor resistance and/or rotor cage asymmetry due to porosity results in degradation in motor efficiency, torque pulsation, and unbalanced magnetic pull that causes increased vibration [1]-[6]. It also can cause important motor characteristics such as the starting performance or torque-speed characteristics to deviate significantly from what is specified by the motor manufacturer. Although degradation in motor performance and reliability can be tolerated for low voltage, low output motors, it is a major concern for motors with high output power ratings.

Quality assurance testing of porosity can be performed by measuring the weight of the rotor before and after die-casting to screen out the relatively light units that are likely to have high porosity levels (or low Al fill factor (FF)), as shown in Fig. 1(b)-(c). However, it is not suitable for quality assurance testing because of the high cost, and it is only used for qualification of the die cast process and rotor design. It is also possible to observe the porosity level and distribution with X-ray scanning; however, it is only suitable for testing of a selected representative sample to qualify die cast process and design due to the excessively high cost [6]. Balancing of the rotor is performed on all rotor units after manufacturing to prevent vibration produced due to rotating unbalance in the rotor. Although the purpose of balancing is not porosity detection, concentrated balancing weights can provide an indirect indication of concentrated porosity.

Many off-line and on-line tests have been devised and have become commercially available for evaluating rotor cage asymmetry to improve motor performance and reliability [7]-[10]. Most of the research and development effort have been focused on detecting faults in the field when the motor is in-service, and not for quality assurance or porosity testing. The test methods have advantages and disadvantages in terms of sensitivity, reliability, ease of testing, etc, for the different types of rotor defects. In general, on-line testing based on *motor current signature analysis* (MCSA) or assembled off-line test methods such as the *single-phase rotation test or rotor influence check* lack sensitivity since they rely on observing the asymmetry in the rotor indirectly from the stator [9]-[12]. They are not suitable for detecting minor porosity or distributed

(a) (b) (c)

Fig. 1 Example of (a) porosity in the end ring of an Al die cast rotor; and measurement of rotor weight (b) before and (c) after die-casting to estimate the porosity level

porosity that do not produce asymmetry. In addition, the requirement of insertion of the rotor into the stator and/or loading of the motor makes it difficult to apply them at motor manufacturing or repair facilities. Disassembled off-line rotor test methods such as the growler or rated rotor flux tests can provide sensitive detection of localized rotor faults since the rotor cage condition is observed directly from the rotor surface. The growler test excites the rotor bars with a U-shaped electromagnet fed by a 60 Hz ac source [9]-[10], and senses the flux produced by the induced bar current using a hacksaw blade or magnetic viewing film to detect open circuit bars. However, it is a pass/fail test incapable of providing a quantitative measure of minor or distributed porosity that are below the threshold level of the detector. In addition, safety risks during testing due to electric shock or arcing are present due to the voltage levels applied [10]-[16].

New off-line test methods intended for detecting anomalies in die-cast or fabricated rotor cages that overcome the problems of conventional test methods summarized above have been recently proposed in [13]-[16]. In [13], a permanent magnet based dc injection probe excites the rotor bars while the rotor is manually rotated. A flux sensing coil on the injection probe senses the anomaly in the flux pattern caused by the low bar current due to defects in the rotor cage. It is shown that major defects such as open circuit Al die-cast bars can be detected; however, detection of minor or distributed porosity or rotors with low FF is not investigated. In [14]-[16], a growler test probe is used for injection of 60 Hz flux while the rotor is manually rotated. A separate flux sensing probe is installed to measure the flux produced by the current excited in the bar to provide a quantitative indication of asymmetry in the cage. It was shown that contact problems in fabricated copper bars could be detected with high sensitivity. However, the sensitivity to distributed porosity or low FF in Al die cast rotors have not been tested. In addition, there were some sensitivity issues for closed slot rotors due to the influence of the slot bridge on excitation and sensing. In this paper, a new off-line test method that focuses on detecting Al die-cast rotor porosity based on electromagnetic flux injection with simplified hardware is proposed. The feasibility of the proposed approach is verified through 3 dimensional (3D) finite element analysis (FEA) and experimental testing on rotors of a 5.5 kW motor using a growler tester under controlled porosity conditions that are difficult to detect with conventional test methods.

II. Porosity in Al Die-cast Squirrel Cage Rotors

The fill factor (FF) of a die cast rotor is defined as the ratio between the actual volume and the intended (ideal) volume of the conductor material used in the rotor cage in percent (%). The FF of Al die-cast rotors is typically between 85% to 99%, and depends on the rotor size, die casting method, and the conditions on temperature, pressure, and speed (in case of centrifugal casting) applied [5]. The normal distribution of the FF of Al die cast cage rotors of a 440 V, 15 kW induction motor was estimated by measuring the weight of 64 rotor samples, as shown in Fig. 2 [6]. The average FF and standard deviation were calculated as 97.1% and 0.76, respectively. Although the FF of only 64 samples were measured, the variance in the individual samples was evident.

The distribution of porosity within the rotor cage of a 440 V, 15 kW and 1.5 kW induction motors was also observed with an x-ray scan [6]. The bars and end rings were scanned in the axial direction after removing the end rings from the rotors. The scan results of the bars at a single axial position in the center of the slots are shown in Figs. 3(a), 4(a) for the 15 kW and 1.5 kW rotors, respectively, where the black part in the center of the bars represent porosity (air). It can be seen in both figures that that porosity is concentrated in the center part of the bars, and cannot be observed near the bar surface. The scan results of the end ring near the axial center of the end ring, and at an axial position close to the rotor core are shown in Fig. 4(b)-(c), respectively. The scans show that porosity in the end ring is concentrated on the inside near the rotor core where the rotor bars are located, and in the center of the ring in the radial direction. Porosity in the interface between the bar and end ring, where the current density is high, could have a significant impact on the equivalent rotor resistance, and influence the motor torque characteristics. As in the case of the bars, porosity could not be observed in the surface of the end ring.

Porosity in the end ring can be observed more clearly in the

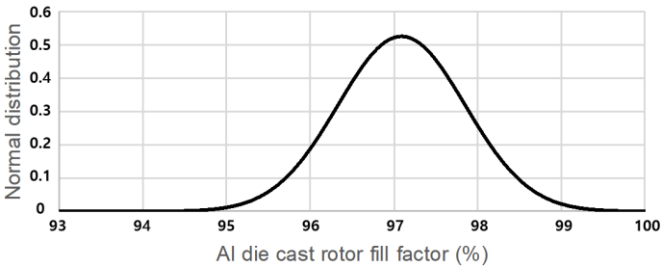

Fig. 2 Normal distribution of fill factor (FF) estimated based on weight measurement of 64 Al die cast rotor samples of 440 V, 15 kW motor

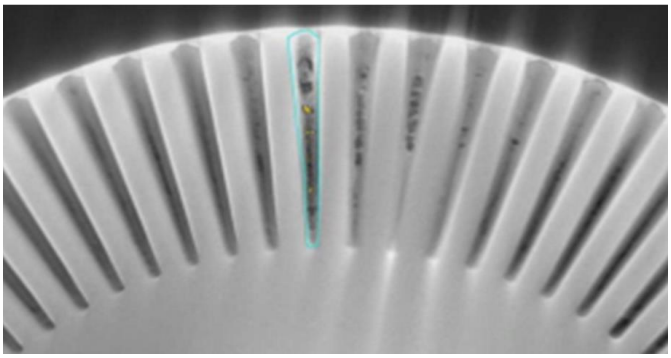

(a)

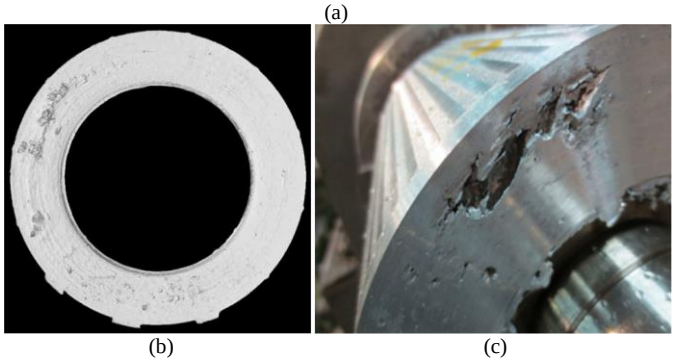

(b) (c)

Fig. 3 X-ray scan of (a) rotor bars in the center of the slot (in the axial direction); (b) 3D reconstruction of the 2D x-ray scan of the end ring; and (c) cut cross section of end ring for a 440 V, 15 kW Al die cast induction motor

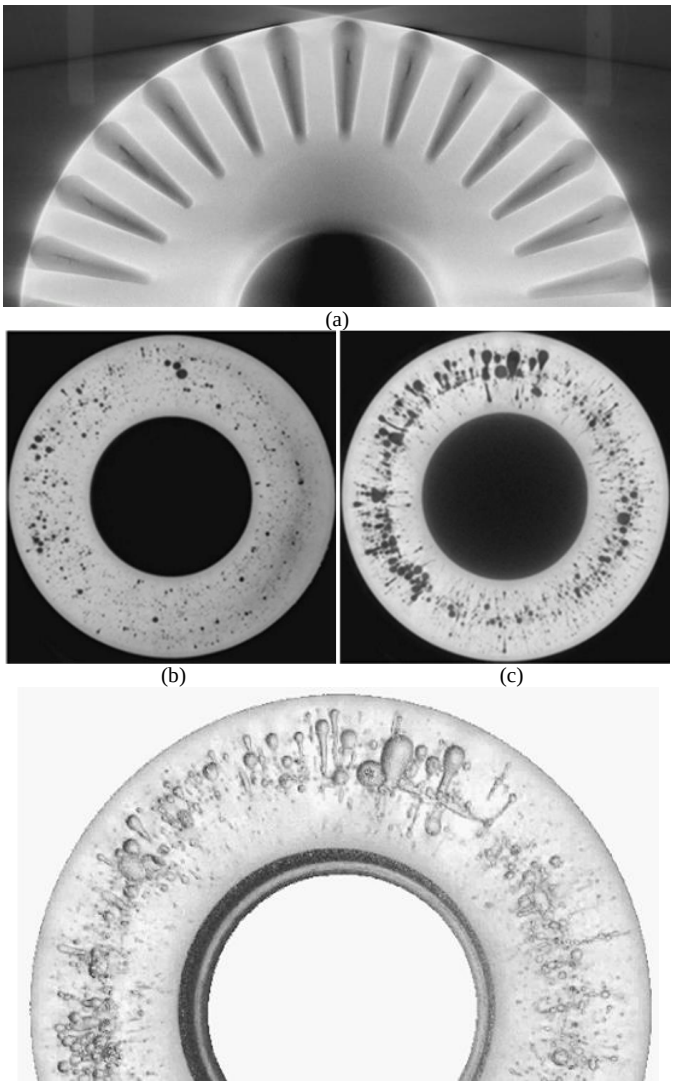

Fig. 4 X-ray scan of (a) rotor bars in the center of the slot (in the axial direction), (b) axial center of end ring, (c) end ring near the rotor core, and (d) 3D reconstruction of the 2D x-ray scan of the end ring shown in (b)-(c) for a 440 V, 1.5 kW Al die cast induction motor

3D reconstruction plots of the 2D end ring x-ray scans in Figs. 3(b) and 4(d) for the 15 kW and 1.5 kW rotors, respectively. The 3D plots show that the overall porosity level is low in the end ring for the 15 kW rotor, where concentrated porosity can be observed. For the 1.5 kW rotor, porosity is spread out with a high overall porosity level. One of the end rings of the 15 kW unit was cut to observe the cross section to confirm the presence of concentrated porosity observed with the x ray scan, as shown in Fig. 3(c). The x-ray scan results show that porosity usually not observable from the rotor surface, is present throughout the bar and end rings, and can have a significant impact on motor performance and reliability.

III. Concept of Proposed Quality Assurance Test

The proposed quality assurance test for screening out defective rotors with minor and distributed porosity in the rotor cage is an off-line test performed on the rotor before insertion into the stator. The test method utilizes a growler tester, which is available in most manufacturing or repair facilities, where flux is directly injected into the rotor surface to excite the rotor bars. The test is performed in a way similar to the methods presented in [13]-[16], where the growler tester excites the rotor bars locally while the rotor is turned manually or automatically at low speed, as shown in Fig. 5. The balancing machine can serve as the platform for rotating the rotor with the electromagnetic flux injection probe fixed for maintaining constant airgap between the probe and rotor. The proposed test can be used for screening out defective rotors during rotor balancing since it is performed on all rotors at the end of the manufacturing stage. The flux injection probe consists of a U-shaped ferromagnetic core with multiple-turn excitation windings for producing the MMF required for flux injection. It is used for both 1) exciting the bars and end rings with ac voltage applied and for 2) extracting the information on rotor porosity by processing the coil voltage and current measurements. This simplifies the hardware requirements when compared to [13]-[16], since an existing growler exciter can be used, and a separate flux sensor or a permanent magnet is not required. It is also capable of extracting information with higher sensitivity than existing methods regarding the rotor condition since the resistive and reactive components can

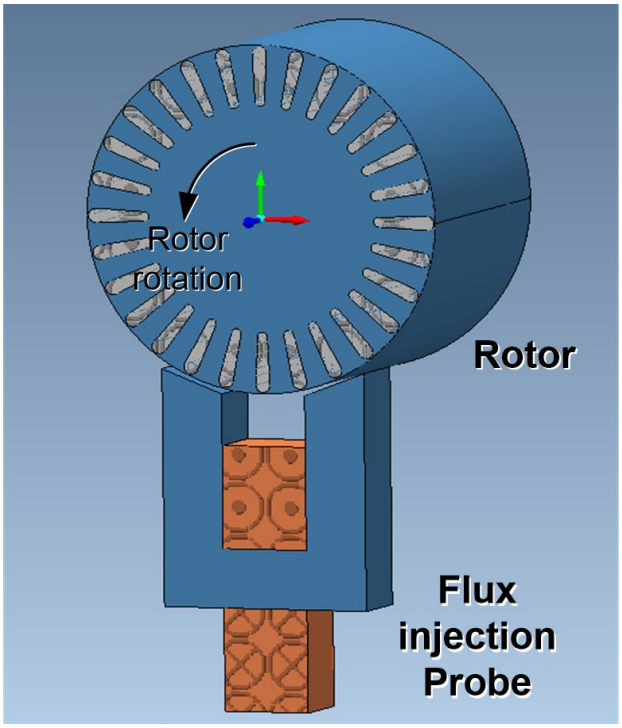

Fig. 5 Test setup of proposed rotor cage quality assurance test

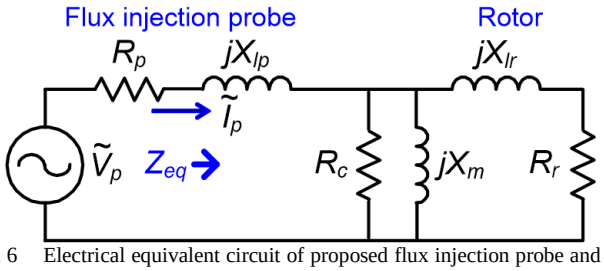

Fig. 6 Electrical equivalent circuit of proposed flux injection probe and the rotor slots under excitation

be separated, as will be described below.

The electrical equivalent circuit of the flux injection probe and the rotor under testing can be derived as shown in Fig. 6. The resistance and leakage reactance of the flux injection probe coil are represented as R_p and X_{lp}, the magnetizing reactance of the flux probe coil is X_m, and the core loss in the system is taken into account with R_c. The equivalent leakage reactance and resistance of the rotor cage under excitation with the flux injection probe are represented as X_{lr} and R_r, respectively. The equivalent impedance, Z_{eq}, can be calculated from the applied voltage, $\mathbf{V_p}$, and current, $\mathbf{I_p}$, phasors as

$$Z_{eq} = \mathbf{V_p} / \mathbf{I_p} - R_p = R_{eq} + jX_{eq}, \quad (1)$$

where R_{eq} and X_{eq} are the equivalent resistance and reactance, respectively. Since it is the change in equivalent impedance with rotor rotation that is being monitored, the equivalent resistance of the flux injection probe, R_p, is subtracted to improve the sensitivity of porosity detection. It should be noted that the equivalent circuit of Fig. 6 is intended to provide a qualitative description of the proposed method. A linear circuit is not accurate due to non-ideal factors such as magnetic saturation, deep bar and skin effect.

When the bar with porosity passes the flux injection probe as the rotor is rotated, the equivalent R_r increases since porosity causes increase in the rotor cage equivalent resistance. This causes local increase in R_{eq} when plotted as a function of rotor position allowing local porosity in the rotor to be detected. Porosity will also cause variation in other equivalent circuit parameters as well, and therefore, both R_{eq} and X_{eq} can vary depending on the rotor design. However, it was observed that porosity mainly causes a local increase in R_{eq}, and therefore, monitoring of R_{eq} can provide a sensitive indication of porosity.

The proposed test method provides higher sensitivity in detecting porosity since the R_{eq} and X_{eq} components can be monitored separately. Irregularities in the rotor surface introduced during lamination punching, leakage of aluminum or rotor eccentricity/ovality that cause variation in the probe-rotor airgap has a significant impact on X_{eq} especially for closed slot rotors. If the total flux amplitude is measured as in [13]-[16], there is no means of separating porosity and rotor surface irregularities. Another advantage of the proposed test method is that it can detect local porosity concentrated in the individual slots. It was reported in a number of resources that N rotor faults distributed 180/N electrical degrees apart do not produced asymmetry, and are not observable with on-line MCSA, off-line single-phase rotation, or rotor influence check tests that rely on detecting the "electrical asymmetry" in the rotor [8]. Porosity is very likely to produce this type of defect, and can be detected with the proposed method since the individual bars are scanned. It is possible that porosities too small to be detected with testing are distributed evenly all over the Al die cast cage, and do not produce asymmetry. This type of defect that decreases the FF can also be detected by monitoring the relative amplitude of R_{eq}. The value of R_{eq} measured with the proposed method is expected to be higher for rotors with higher porosity levels (or lower FF).

The excitation voltage and frequency can be optimized to provide high sensitivity in detecting the fault of interest for the type of rotor slot design. It can be predicted that excitation frequency below the rated frequency can provide sensitive detection of rotor faults since penetration of flux into the rotor yoke is advantageous. In addition, lower excitation frequency provides lower sensitivity to airgap variations due to surface irregularities. With high excitation frequency, flux penetration is limited due to rotor cage eddy current rejection. If the flux is concentrated on the rotor surface, the equivalent impedance is not influenced by the rotor and mainly becomes a function of the airgap (X_m). For rotors with closed rotor slot design, it may be difficult to observe increase in R_{eq} due to porosity since the flux takes minimum magnetic reluctance path through the rotor slot bridge. However, if the voltage level is increased, the slot bridge can be saturated to push the flux beyond the slot bridge to improve the sensitivity of porosity detection.

IV. 3D Finite Element Analysis

Since using the electrical equivalent circuit cannot provide sufficient accuracy, a 2D time harmonic FEA was attempted. However, the flux in the axial direction from the probe could not be taken into account resulting in insufficient accuracy. Therefore, a 3D time-harmonic FEA was performed as it provided reasonable accuracy. A 3D model of a 380 V, 5.5 kW, closed slot aluminum die cast rotor with 28 rotor slots, shown in Figs. 5 and 7, was used to verify the proposed test concept. This rotor is identical to rotor B1 used in V for experimental verification. 3D FEA was used for simulating the flux injection probe based test under controlled fault conditions and for determining the excitation conditions suitable for sensitive detection of porosity faults. A 300 turn probe similar to the prototype used for experimental verification in V was used for flux injection in the FEA (R_p=0.2716 Ω at 50 Hz). The airgap between the probe and rotor was set at 1.5 mm to allow for sufficient margin for preventing contact, since surface irregularities due to burrs or leaked aluminum are common.

3D FEA was performed to extract the equivalent circuit parameters, R_{eq} and X_{eq}, for all rotor slots for a rotor with defects introduced in two slots 90 degrees apart. The FF of the rotor cage was assumed to be 100% in the FE study. Porosity at the axial end of the bar was emulated by introducing a 30 mm thick porosity (air) covering half of the bar cross sectional area at the outer portion, as shown in Fig. 7(a). A fully broken bar was also emulated by including 5 mm thick air at the axial end of the bar covering the entire bar area, as shown in Fig. 7(b). The two slots with rotor defects were separated by 7 slots to avoid interference between defects. The rotor was rotated in discrete steps with the probe location fixed. After performing the FE under different excitation conditions, the voltage and

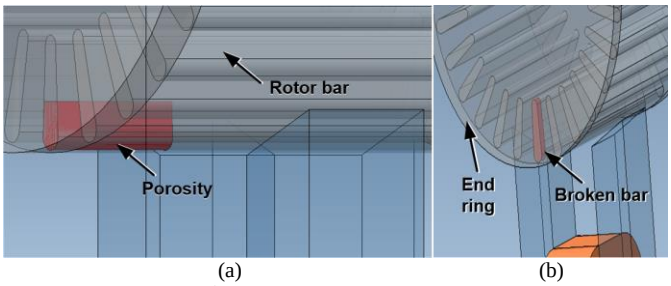

(a) (b)

Fig. 7 3D FE model of rotor bar with emulated (a) porosity; (b) broken bar

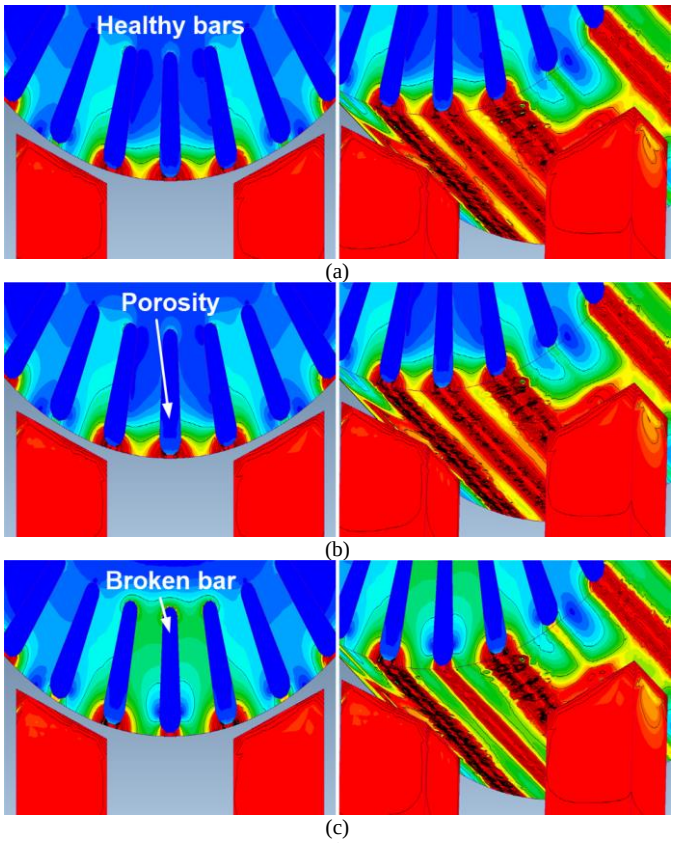

Fig. 8 3D FEA results: magnetic flux distribution under 66 V, 50 Hz excitation with the flux probe enclosing slots with (a) healthy, (b) porosity, and (c) broken bars

frequency for detecting porosity was set at 66 V, 50 Hz. The excitation conditions did not have a significant impact on the detectability or sensitivity of the method as long as the voltage and frequency is within a given range.

The results of the 3D FEA magnetic flux distribution are shown in Figs. 8(b)-(c) with the probe placed to enclose the slot with no defect, porosity, and broken bar. R_{eq} was calculated from the measurements of the applied coil voltage and current from (1). The values of R_{eq} as a function of rotor slot number for the 28 slots are shown in Fig. 9(a). The increase in the value of R_{eq} can be observed when the injected flux is enclosing the defective bars, and the increase in R_{eq} is proportional to the severity of the defect, as predicted. The local variation in the X_{eq} measurements did not convey meaningful information on rotor defects. The simulation results verify that local increase in R_{eq} can provide detection of local porosity defects in the rotor cage.

V. Quantification of Porosity Defects

It can be seen from III-IV that porosity can be detected from the values and pattern of R_{eq}. Although the R_{eq} plot as a function of rotor position can provide a qualitative indication of porosity, it is desirable to define quantitative indicators to establish a consistent standard for screening out defective rotor units with distributed or concentrated porosity and/or low FF. For concentrated porosity, an effective quantitative indicator is to normalize the R_{eq} values with respect to its median value, as shown in Fig 9(b) for the FEA results. The percent increase in the value of the normalized R_{eq} is defined as the ΔR_{eq} and its maximum value is defined as $\Delta R_{eq,max}$. The values of ΔR_{eq} for the defects are 13.3%, 4.9%, respectively for the slot with the broken bar and porosity defined in IV, as shown in Fig. 9(b).

Although ΔR_{eq} can provide sensitive indication of concentrated porosity, it is not sensitive if porosity is distributed evenly in the rotor cage since there is no asymmetry. Since porosity distributed across the cage results in low FF and increase in R_{eq}, the average value of the R_{eq} measurements, $R_{eq,avg}$, can serve as an effective indicator of low FF due to porosity. $R_{eq,avg}$ is intended for screening rotors with low FF, but also increases with concentrated porosity (1.9%) as shown in Fig. 9(a) for the FE simulation results. As the value of R_{eq} depends on the rotor design, the statistical distribution of $R_{eq,avg}$ values from the rotors of identical design must be analyzed to screen out the outliers with high porosity (or low FF) levels. The two indicators, $\Delta R_{eq,max}$ and $\Delta R_{eq,avg}$ can be used for determining the nature and severity of the defective rotor units due to porosity for quality assurance. The validity of the two fault indicators different types and severity levels of porosity is demonstrated in VI.

VI. Experimental Study

A. Experimental Setup

To verify the feasibility of the proposed approach, testing was performed on two types of 380 V, 5.5 kW induction motor rotors with a growler test probe. The probe was fabricated in

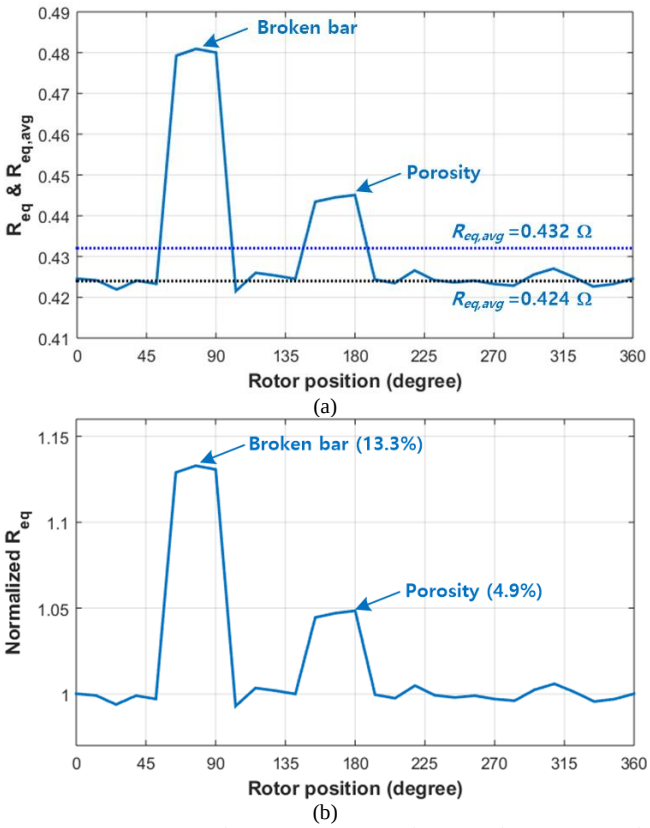

Fig. 9 3D FEA results of normalized R_{eq} as a function of rotor position for broken bar and porosity located at 77 and 167 degrees (66 V, 50 Hz excitation)

the lab to be similar to a commercial growler tester with 300 turns of stranded coil wound on a U-shaped ferromagnetic core, as shown in Fig. 10(a) (R_p=0.5879Ω). Sheets of motor core laminations were cut and attached on the probe surface to make the magnetic flux distribution uniform between the probe and rotor. The test bed shown in Fig. 10(b) was used to rotate the rotor with respect to the center of the shaft while maintaining an airgap of 1.5 mm with the probe fixed on the bottom. A commercial 16 bit data acquisition system was used to digitize the voltage and current measurements at 3 kHz, from which the amplitude and phase angle were extracted for calculation of R_{eq} and X_{eq} from (1).

Testing was performed on a 44 bar semi-open slot rotor (rotor A) and a 28 bar closed slot rotor (rotor B), shown in Figs. 11(a)-(b), respectively, to verify that the proposed quality assurance test works for both types of rotor designs. A number of porosity defects of varying types and severity levels were intentionally inserted in rotors A and B for testing. The capability of the proposed method was tested on 4 rotors with the following defects:

- Rotor A1: 2 adjacent bars broken by drilling holes from the outer surface at the rotor bar and end-ring joint. 100% and 65% of the bar depth removed from the outer surface by drilling a hole. The 2 defective bars are 8 rotor slots apart.
- Rotor A2: 0, 1, and 2 bars broken 90 degrees apart to cancel rotor electrical asymmetry. The bars are broken by drilling holes 90% of the bar depth from the outer surface.

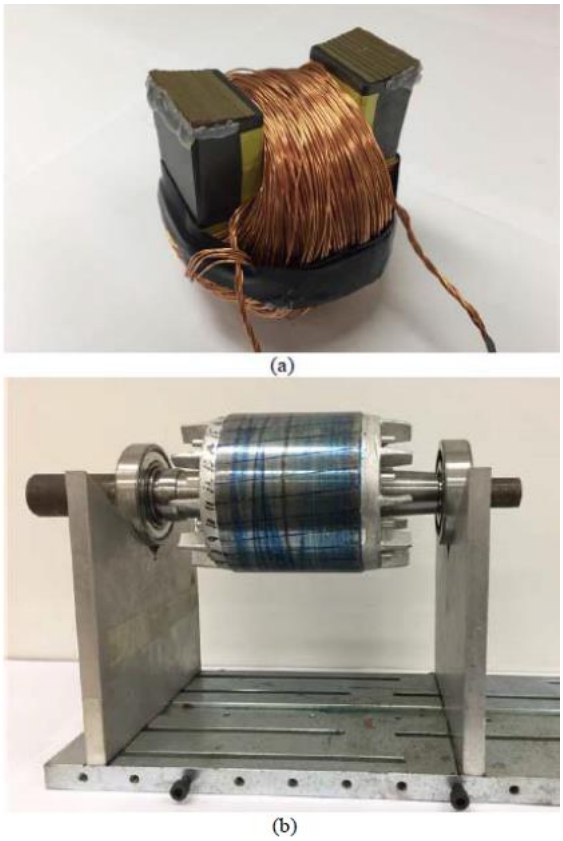

(a) (b)

Fig. 10 Experimental test setup for proposed rotor test method; (a) prototype electromagnetic flux injection probe; (b) test bed for rotor rotation

- Rotor A3: New rotor confirmed with large inherent asymmetry in R_{eq} due to porosity. 0, 11 and 22, 3 mm diameter holes evenly drilled 70% of slot depth on one side of the end ring at bar-end ring interface (Figs. 11(a), 12(a)). This emulates uniformly distributed porosity at locations observed in the Fig. 4(c) x-ray scan. This corresponds to 0%, 0.4%, and 0.8% decrease in FF. The other side of the end ring cut off from the rotor after testing (Fig. 12(b)).
- Rotor B1: 1 bar broken by drilling a hole from the outer surface (Fig 11(b)).

B. *Experimental Results*

The measurements of normalized R_{eq} obtained from the semi-open and closed slot rotors with emulated porosity and broken bars (rotors A1 and B1) are shown in Figs. 13(a)-(b), respectively. The coil was excited at 66 V and 20 V (50 Hz) for the closed and open slot rotors, respectively. A higher voltage level was required for the closed slot rotor, because it is

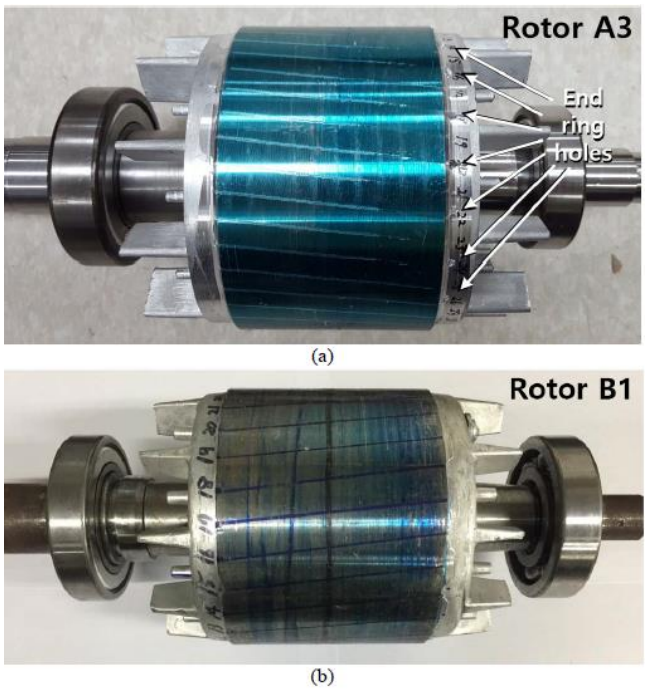

(a) (b)

Fig. 11 (a) 44 bar semi-open slot (rotor A3) and (b) 28 bar closed slot aluminum die cast (rotor B1) rotors used for porosity testing

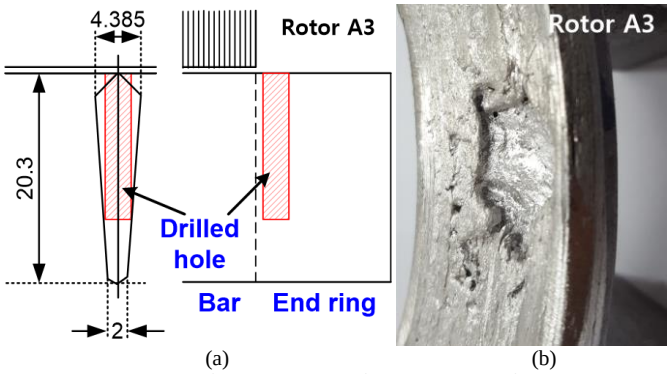

(a) (b)

Fig. 12 (a) Location of end ring holes for emulating unformly distributed porosity (rotor A3), and (b) end ring porosity due to manufacturing defect observed for rotor A3

desirable to saturate the slot bridge for penetration of flux beyond the slot bridge for improving the porosity detection sensitivity. It can be seen in Figs. 13(a)-(b) that a clear increase in R_{eq} proportional to the severity of the damage can be observed when the probe passes the damaged bars. The values of the two ΔR_{eq} peaks are 34.7% and 16.7%, respectively, for rotor A1, and 6.6% for rotor B1. It can also be seen that R_{eq} of the bars is non-uniform when passing the bars without intentional damage, due to non-uniform porosity unlike the ideal case with 100% FF in Fig. 9.

A comparative evaluation of the proposed test with MCSA and the single-phase rotation test was performed for rotor A2, which represents a case where a combination of 2 defects cancels out the asymmetry. MCSA, the single-phase rotation test, and proposed test were performed on rotor A2 1) before fault insertion, 2) after damaging 1 bar, and 3) after damaging another bar 90 electrical degrees apart from the first bar. The results of the 3 tests are shown in Figs. 14(a)-(c). With MCSA, the amplitude of the rotor fault frequency component for a healthy rotor (-56.8 dB) increased to -48.8 dB after breaking 1 bar, as shown in Fig. 14(a). However, it decreased to -54.6 dB after the 2nd bar was broken because the asymmetry cancels for the two defects located 90 electrical degrees apart. It is likely that the rotor would be misdiagnosed as "healthy" causing a false negative alarm with a -54.6 dB indication. The defects could not be clearly observed with the off-line single-phase rotation test, as shown in Fig. 14(b) due to the low sensitivity. The two local defects inserted are clearly observable from the 2 peaks in R_{eq} obtained with the proposed test, as shown in Fig. 14(c), since the individual slots are scanned from the surface. The values of the $\Delta R_{eq,max}$ were 8.6%, 33.4%, and 29.2%, and $R_{eq,avg}$ were 0.691Ω, 0.710Ω, and 0.722Ω, respectively for the cases of 0, 1, and 2 broken bars, which indicates that both fault indicators are higher for the rotor with a defect. The non-uniform R_{eq} pattern of the healthy rotor in Fig, 14(c) shows that there is inherent asymmetry in the rotor due to porosity. It can also be seen that the test results are repeatable for the slots where defects were not introduced. The results for rotor A2 are meaningful since the 2 defects can be detected for a case where existing test methods fail.

For rotor A3, the inherent asymmetry in the normalized R_{eq} measurements was very large compared to that of other rotors.

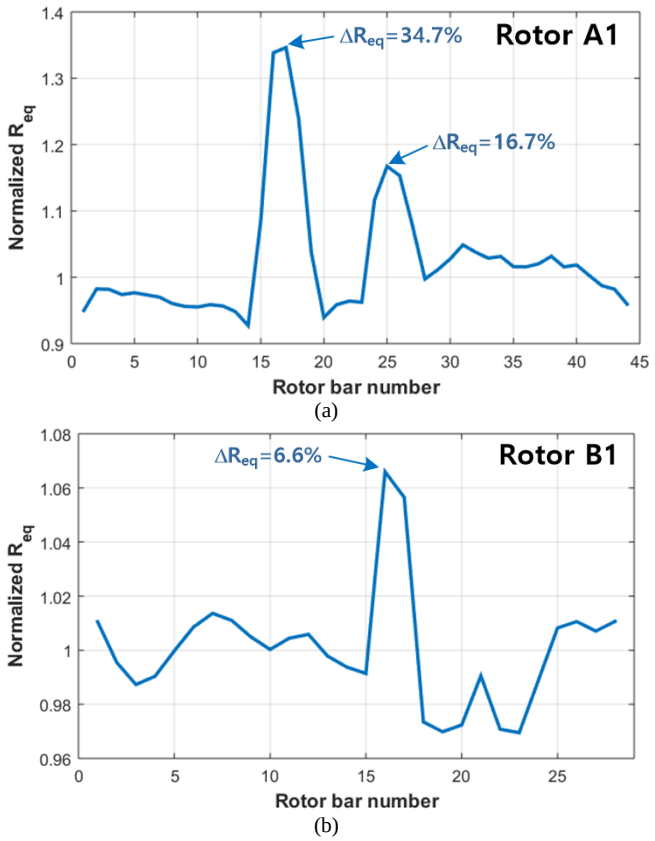

Fig. 13 Normalized equivalent resistance, R_{eq}, measurements of (a) semi-open slot (rotor A3) and (b) closed slot (rotor B1) rotor

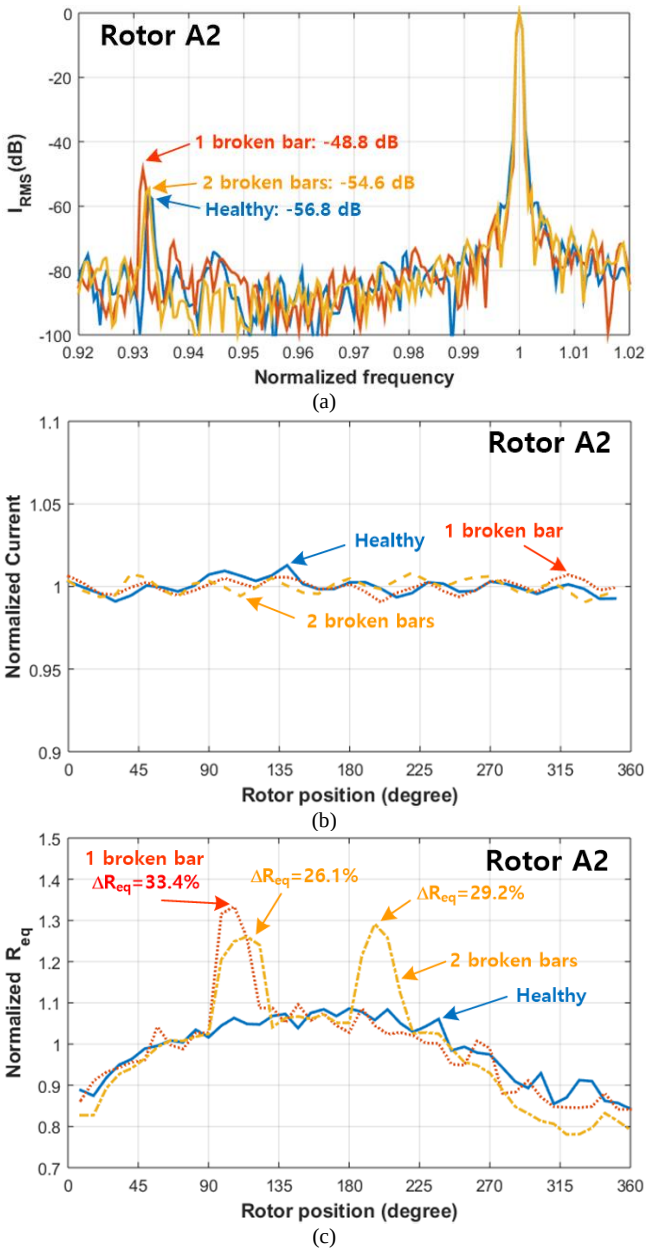

Fig. 14 Comparative test results for the case where 2 broken bars 90 electrical degrees apart cancel out asymmetry (rotor A2): (a) MCSA; (b) single phase rotation test; and (c) normalized R_{eq} measurements of proposed test

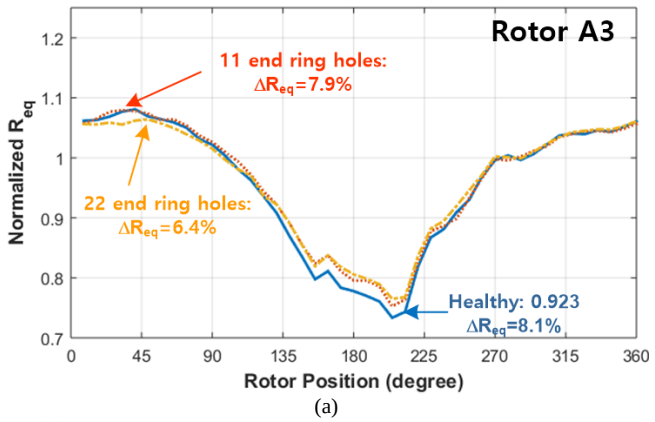

(a)

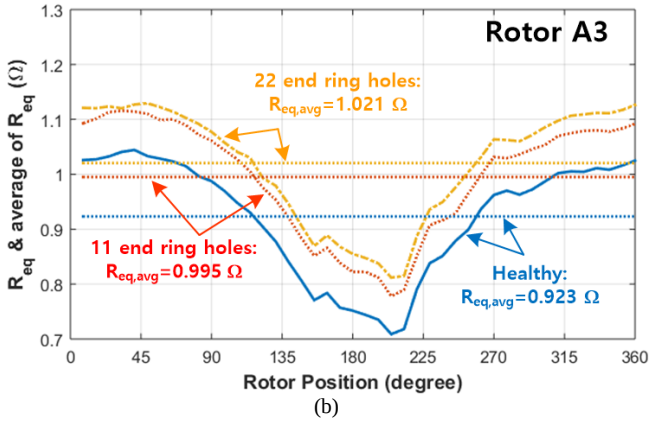

(b)

Fig. 15 (a) Normalized R_{eq}, (b) R_{eq}, and R_{eq},avg measurements for rotor A3 with 0, 11, 22 end ring holes distributed evenly on one side of the end ring (rotor A3)

Table I $\Delta R_{eq,max}$, $R_{eq,avg}$, and $\Delta R_{eq,avg}$ (Increase from $R_{eq,avg}$ value of healthy rotor A2) for rotor samples A1, A2, and A3

Rotor	Defect condition	ΔR_{eq} (%)	$R_{eq,avg}$ (Ω)	$\Delta R_{eq,avg}$ (Ω)
A1	100%, 65% broken bars	34.7	0.741	0.050
A2	Healthy	8.6	0.691	-
	90% broken bar	33.4	0.710	0.019
	Two 90% broken bars	29.2	0.722	0.031
A3	Healthy	8.1	0.923	0.232
	11 holes in endwinding	7.9	0.995	0.304
	22 holes in endwinding	6.4	1.021	0.330

This rotor sample was used to evaluate if the increase in the overall porosity level (or decrease in the FF) could be detected from the average of R_{eq} obtained from the proposed test. For this case, the normalized and actual values of R_{eq} are shown in Fig. 15(a)-(b), respectively. It can be seen in Fig. 15(a) that there is no significant change in the ΔR_{eq} or $\Delta R_{eq,max}$ values since the porosity is evenly distributed (8.1%, 7.9%, and 6.4%). However, the average values of R_{eq} obtained from the cases with 11and 22 evenly distributed end ring holes were 0.995 Ω , and 1.021 Ω , respectively (Fig. 15(b)). This corresponds to a 7.23 % and 10.6 % increase from the case without end ring holes (R_{eq}=0.923Ω). This is a significant increase considering that only 0.4% and 0.8% of the Al material was removed. The values are also significantly higher compared to that of rotor A1 and A2. The value of R_{eq} for a healthy rotor A3 is higher than that of the healthy rotor A2 by 0.232Ω, which indicates that the level of inherent porosity is very high in rotor A3. The results show that the overall porosity level (or rotor FF) can be monitored for screening out defective units in addition to detecting local porosity defects, as in the cases of rotors A1, A2, and B1. A large porosity in the end ring that spans more than 2 rotor slots was observed on the other side of the end ring of this rotor, as shown in Fig 12(b). It is suspected that this is the likely cause of the large inherent asymmetry.

The values of $\Delta R_{eq,max}$ and $R_{eq,avg}$ for rotors A1, A2, and A3 of identical design, are summarized in Table I. By comparing the two fault indicators with respect to the relatively healthy case of rotor A2, it can be seen that there is a significant increase in $\Delta R_{eq,max}$ for concentrated porosity, and an increase in $R_{eq,avg}$ for cases where the porosity level is higher. The difference between $R_{eq,avg}$ and the healthy case of rotor A2 for all cases are also shown in the right end column of Table I to show the relative porosity levels. The results of Figs. 13-15, and Table I demonstrate that rotors with concentrated or distributed porosity can be detected with the proposed method and fault indicators to screen out defective rotor units with high porosity levels.

VII. Conclusion

An off-line quality assurance test method for screening out aluminum die cast rotor units with porosity was proposed in this paper. The proposed flux injection probe can be used to excite the individual rotor bars to obtain information on porosity during post-manufacturing balancing of rotors. 3D FEA and experimental test results showed that the new test method can be used for obtaining a quantitative measure of individual rotor bar condition for screening out rotors with high porosity levels. This allows sensitive detection of rotors with porosity whether they are concentrated or distributed for both closed and open slot rotors. It was shown that distributed porosity not observable with existing test methods can be detected clearly. Although the focus of the proposed method was on porosity, detection of non-uniformity in the rotor due to eccentricity or ovality is being investigated to extend the capabilities of the proposed quality assurance test.

The proposed test method can be also applied to detecting defects in fabricated copper rotors due to brazing imperfection, cracks, broken bars, etc. In addition to quality assurance, it can be used for verification of repair, or periodic testing at manufacturing and repair facilities. It is expected to help prevent low performance motor operation, accelerated degradation, and costly forced outages due to rotor defects.

References

[1] A.H. Bonnett, and T. Albers, "Squirrel-cage rotor options for AC induction motors," *IEEE Trans. Ind. Appl.*, vol. 37, no. 4, pp. 1197-1209, July/Aug. 2001.

[2] S. Williamson, R.C. Healey, J.D. Lloyd, and J.L. Tevaarwerk, "Rotor cage anomalies and unbalanced magnetic pull in single-phase induction motors," *IEEE Trans. on Ind. Appl.*, vol. 33, no. 6, pp. 1553-1562, Nov./Dec. 1997.

[3] W.R. Finley, and M.M. Hodowanec, "Selection of copper versus aluminum rotors for induction motors," *IEEE Trans. on Ind. Appl.*, vol. 37, no. 6, pp. 1563-1573, Nov/Dec 2001.

[4] J.H. Dymond and R.D. Findlay, "Some commentary on the choice of rotor bar material for induction motors," *IEEE Trans. on Energy Convers.*, vol. 10, no. 3, pp. 425-430, Sept. 1995.

[5] H.J. Ahn, K.W. Kim, J.H. Choi, E.S. Kim, Y.C. Lim, “Rotor design for an efficient single-phase induction motor for refrigerator compressors,” *Energies*, vol. 9(3) 158, pp. 1-16, Mar. 2016.

[6] J. Yun, S. Lee, M. Jeong, S.B. Lee “Influence of die-cast rotor fill factor on the starting performance of induction machines,” *Proc. of Compumag*, June 2017.

[7] W.T. Thomson, and M. Fenger, “Current signature analysis to detect induction motor faults,” *IEEE Ind. Appl. Mag.*, vol. 7, no. 4, pp. 26-34, July/Aug. 2001.

[8] S.B. Lee, D. Hyun, T. Kang, C. Yang, S. Shin, H. Kim, S. Park, T. Kong, H. Kim, “Identification of false rotor fault indications produced by on-line MCSA for medium voltage induction machines,” *IEEE Trans. on Ind. Appl.*, vol. 52, no.1, pp. 729-738, Jan./Feb. 2016.

[9] G.C. Stone, I. Culbert, E.A. Boulter, and H. Dhirani, *Electrical insulation for rotating machines – design, evaluation, aging, testing, and repair*, IEEE Press Series on Power Eng., John Wiley and Sons, 2014.

[10] T. Bishop, “Squirrel cage rotor testing,” *Proc. of EASA Conv.*, June 2003.

[11] D. Hyun, S. Lee, J. Hong, S.B. Lee, S. Nandi, “Detection of Airgap Eccentricity for Induction Motors using the Single Phase Rotation Test,” *IEEE Trans. on Energy Convers.*, vol. 27, no. 3, pp. 689-696, Sept. 2012.

[12] T. Kang, J. Kim, S.B. Lee, and C. Yung, "Experimental evaluation of low voltage off-line testing for induction motor rotor fault diagnostics," *IEEE Trans. on Ind. Appl.*, vol. 51, no. 2, pp. 1375-1384, Mar./Apr. 2015.

[13] S.W. Clark, and D. Stevens, “Squirrel cage induction motor cast rotor defect detection with magnetic field analysis,” in *Proc. Int. Conf. Elect. Mach. Syst. (ICEMS’15)*. Oct. 25–28, 2015.

[14] S. W. Clark, “A new method of testing rotor bars,” *Elect. Apparatus*, vol. 68, pp. 29–33, Sep. 2015.

[15] S.W. Clark, D. Stevens, “Induction motor rotor bar damage evaluation with magnetic field analysis,” *IEEE Trans. Ind. Appl.*, vol. 52, no. 2, pp. 1469-1476, Mar./Apr. 2016.

[16] S.L. Nau, *et. al.*, “Methods to evaluate the quality of stator and rotor of electric motors,” *Proc. of IEEE SDEMPED*, pp. 64-70, Aug. 2015.

[17] M. Jeong, J. Yun, Y. Park, S.B. Lee, K.N. Gyftakis, “Off-line flux injection test probe for screening defective rotors in squirrel cage induction machines,” *Proc. IEEE SDEMPED*, pp. 233-239, Sept. 2017.